A Nonisothermal Fourier Transform Infrared Degradation Study of Nitrocelluloses Derived from Wood and Cotton

JEAN-JACQUES JUTIER, YVES HARRISON, STÉFANE PREMONT, and ROBERT E. PRUD'HOMME, *Groupe de recherche sur les macromolécules, Département de chimie, Université Laval, Québec (Québec) Canada G1K 7P4*

Synopsis

The nonisothermal decomposition of nitrocellulose (NC) films cast from acetone, tetrahydrofuran, and ethyl acetate was followed using Fourier transform infrared (FTIR) spectroscopy. NC samples were derived from wood (two samples) and from cotton (four samples) and their nitrogen content ranged from 12.6 to 13.5%. Kinetic parameters such as activation energies and pre-exponential factors were calculated using the curve-fitting treatment initially proposed by Eisenreich and Pfeil and the FTIR relative absorbance intensity of two functional groups (i.e., C=O and NO_2). The experimental data were best described by a first-order autocatalytic equation with activation energies equal to 178 and 175 kJ/mole for the two steps of the autocatalytic reaction. No variation in activation energy was observed between the different NC samples, whatever their nitrogen content and vegetal origin, or the solvent used to cast films. The extinction coefficient of the hydroxyl groups of NC was also determined using a modified Beer-Lambert equation and used to calculate precisely their nitrogen content.

INTRODUCTION

Several aspects of the thermal decomposition of nitrocellulose (NC) have been investigated over the years.[1] Wolfrom et al.[2] studied the thermal decomposition of a cellulose nitrate propellant, under ignition conditions and low pressures, and suggested an homolytic scission of the O—NO_2 bond leading to a solid residue identified as a fragmented type of nitrated oxycellulose having a very low degree of polymerization.

Using differential scanning calorimetry (DSC) and bomb calorimetry, Lemieux and Prud'homme[3] compared the thermal decomposition behavior of several highly nitrated NC derived from cotton and from wood and observed that the average heats of decomposition and explosion of dried NC fibers increase slightly, whereas the average heat of combustion decreases slightly with nitrogen content. The combustive action of oxygen and the inhibitory effect of nitrogen toward NC degradation were discussed.

The analysis of thermal degradation of NC can also be carried out by infrared (IR) spectroscopy. For example, Phillips et al.[4] showed that the kinetics of isothermal decomposition of NC is best approximated by a first-order curve with, however, two or three branches. Typical values of the activation energy and pre-exponential factor are 188.4 kJ/mole and 3.54 10^{10} s^{-1}, respectively, and these values are of the same order of magnitude as those obtained by thermogravimetry. The overall features of the IR spectra suggest

Journal of Applied Polymer Science, Vol. 33, 1359–1375 (1987)
 CCC 0021-8995/87/041359-17$04.00

that the basic structure of the carbon skeleton of NC does not change drastically during the decomposition.

On the other hand, Eisenreich and Pfeil[5] studied by IR spectroscopy highly nitrated NC (13.3% N) decomposed and quenched at different temperatures. They used a curve-fitting procedure to follow the evolution of the IR bands of specific functional groups (i.e., C=O, NO_2, and OH), after normalization with respect to the CH_2 group intensity band, and they found that the best fit was obtained with a first-order autocatalytic equation followed by a second-order simple equation. In this analysis, the autocatalytic process was characterized by two activation energies ranging between 167.9 and 178.3 kJ/mole and between 164.9 and 169.7 kJ/mole, respectively.

In this study, the nonisothermal decomposition of six highly nitrated NC samples derived from wood and from cotton is followed as a function of temperature using Fourier transform infrared (FTIR) spectroscopy. Changes in the FTIR spectra are investigated using samples cast from tetrahydrofuran (THF), acetone, and ethyl acetate. The kinetic parameters of the decomposition reaction are calculated by the Eisenreich and Pfeil's curve-fitting procedure. The extinction coefficient of the hydroxyl groups of NC are also determined using a modified Beer-Lambert equation and used to calculate precisely the degree of substitution of NC.

EXPERIMENTAL SECTION

Materials

Six nitrocellulose samples have been used in this study. Their main characteristics are given in Table I. It should be noticed that the acronym NCW-1342 stands for a nitrocellulose (NC) derived from wood (W) and containing 13.42% of nitrogen; the acronym NCC-1260 stands for a nitrocellulose (NC) derived from cotton (C) and containing 12.60% of nitrogen; the other acronyms have a similar meaning.

The NC wet fibers were dried in a vacuum oven for several days at room temperature. NC solutions (1% by weight) were prepared using freshly distilled THF, spectroscopic grade acetone or ethyl acetate, with dry fibers, and films were cast thereof. In all cases, solvent evaporation was conducted at room temperature unto KBr windows, a petri dish being placed over each window in order to favor the uniformity of the films. The films were then transferred to a vacuum dessicator, kept at room temperature, for 48 h to remove residual solvent. After this treatment, no trace of solvent could be detected on the FTIR spectra.

IR Spectroscopic Technique

Infrared spectra of NC films were obtained using a Bomem DA 3.02 FTIR spectrometer equipped with mercury cadmium telluride and deuterated triglycine sulfate detectors. The frequency scale was calibrated internally with a reference helium–neon laser to an accuracy of 0.001 cm^{-1} at 2000 cm^{-1}. The NC films were sufficiently thin to ensure that the spectral information required was in a range where the Beer-Lambert law is obeyed.[6]

TABLE I
Nitrocellulose Samples Used

Sample	Country of origin	Cellulose source	%N	Molecular weight (GPC) (kg/mole)		Remarks
				$\overline{M_w}$	$\overline{M_n}$	
NCW-1342	Canada	Wood	13.42	405	117	High Grade (Grade B) Expro Chemical Products Inc.
NCW-1262	Canada	Wood	12.62	342	145	Pyro (Grade A, type I) Wood pulp (Rayonier Q-LD) Expro Chemical Products Inc.
NCC-1350	United States	Cotton	13.50	323	103	High grade (Grade B) U.S. Army Ballistic Research Laboratories
NCC-1314	Canada	Cotton	13.14	360	163	Military Blend (Grade C, Type I) Sheeted cotton linters (Buckeye Corp.) Expro Chemical Products Inc.
NCC-1274	Australia	Cotton	12.74	309	125	Mechanically nitrated papered cotton linters (Shoalhaven) Mulwala Explosives Factory
NCC-1260	United States	Cotton	12.60	370	100	Pyro (Grade A, Type I) U.S. Army Ballistic Research Laboratories

The frequency of the FTIR bands was determined by the method of the center of gravity.[7] The intensity values of the various absorption bands were measured in absorbance units with a baseline method. For that purpose, a straight line was drawn between two points located before and after the band or the group of bands under consideration.

NC films were placed between two KBr windows, and then inserted into a thermoregulated cell, where the temperature was continuously monitored (± 0.5K) using an Omega digital readout Model D-921. A copper constantan thermocouple was placed between the two KBr windows, as near as possible to the NC film. Films were decomposed between 320 and 500 K under 1–2 mm pressures at a heating rate of 0.5 K/min. At selected temperatures, 90 scans were recorded at a resolution of 2 cm^{-1}, signal-averaged, and stored on a magnetic disk. To determine the extinction coefficient of the OH groups, 100 scans were recorded at room temperature with a resolution of 2 cm^{-1} and signal-averaged. A dry nitrogen flow was continuously maintained over the films and used as a purge throughout the measurements. A Beer-Lambert law relationship was assumed between the concentration of functional groups and band absorbance.

Kinetics

The kinetic parameters (activation energies E_1 and E_2 and pre-exponential factors Z_1 and Z_2) of the decomposition reaction were determined by the curve-fitting procedure proposed by Eisenreich and Pfeil.[5] The equations used assume a first-order autocatalytic reaction, followed by a simple order kinetics. Under nonisothermal conditions, the autocatalytic reaction is described by the differential equation:

$$\beta\, d\alpha/dT = -k_1(T) - k_2(T)\alpha(1-\alpha) \tag{1}$$

where β is the linear heating rate, α the experimental IR absorbance variation of a specific functional group, k_1 is the first-order rate constant, and k_2 that of the autocatalytic reaction. $k_1(T)$ and $k_2(T)$ are defined by:

$$k_i(T) = Z_i \exp(-E_i/RT) \tag{2}$$

The solution of Eq. (1) is:

$$\alpha(T) = \frac{\exp\{-[(Z_1/\beta)S_1(T) + (Z_2/\beta)S_2(T)]\}}{1 - (1/\beta)\int_{T_0}^{T} k_2(T)\exp\{-[(Z_1/\beta)S_1(T) + (Z_2/\beta)S_2(T)]\}\, dT} \tag{3}$$

where $S_1(T)$ and $S_2(T)$ are the integrals of the Arrhenius function:

$$S_1(T) = \int_{T_0}^{T} \exp(-E_1/RT)\, dT \tag{4}$$

$$S_2(T) = \int_{T_0}^{T} \exp(-E_2/RT)\, dT \tag{5}$$

(E_1, Z_1) and (E_2, Z_2) are the activation energies and pre-exponential factors of the monomolecular and catalyzed reactions, respectively. $S(T)$ was calculated using the first five terms of a semiconvergent series[8] and the integral involved in Eq. (3) was computed numerically using Simpson's rule.

The nth order simple kinetic reaction is described by the equation:

$$\beta\, d\alpha/dT = -k_n(T)\alpha^n \tag{6}$$

where $k_n(T)$ is the rate constant of the decomposition process defined by Eq. (2). The solution of Eq. (6) is:

$$\alpha(T) = [1 + (n-1)\beta Z S(T)]^{1/(1-n)} \tag{7}$$

The kinetic parameters for the degradation of NC films were determined by fitting Eq. (3) and Eq. (7) to the experimental data using a nonlinear least-squares program.[9] With first-order simple kinetics, one can describe, in the best cases, only the very beginning, corresponding to a decrease (or increase) of about 10% in the band intensity, of the IR absorbance versus temperature curve.

RESULTS AND DISCUSSION

NC FTIR Analysis

Figure 1 shows the FTIR spectrum, taken under nitrogen atmosphere between 480 and 4000 cm^{-1}, of a NCW-1262 film cast from THF.

The frequencies, relative intensities, and assignments of most of the absorbance bands of the FTIR spectrum of NC in the 480–4000 cm^{-1} region are summarized in Table II.

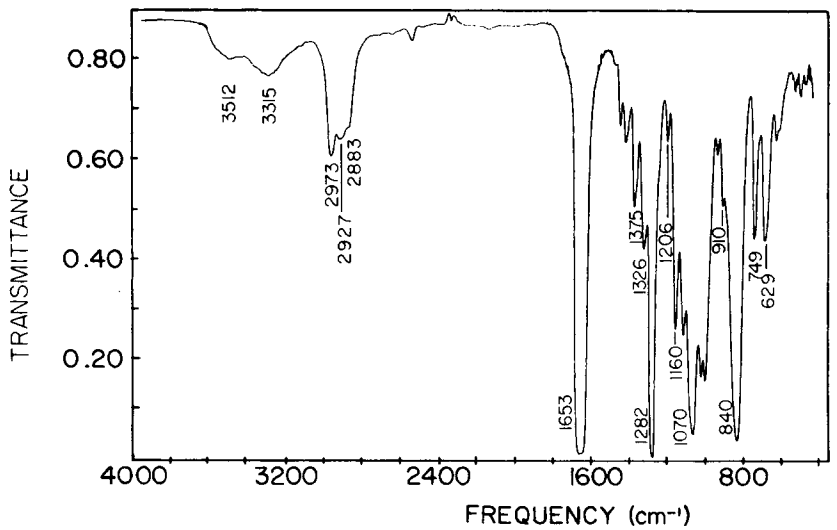

Fig. 1. FTIR spectrum in the 480–4000 cm^{-1} region of a NC film (NCW-1262) cast from THF at 298 K under nitrogen atmosphere. (Spectrum taken on a thick film in order to blow up the intensity of the smaller bands for illustration purposes.)

TABLE II
FTIR Spectrum of Nitrocellulose

Frequency (cm^{-1})	Relative intensity[a]	Assignment
3512	w	OH stretching
3315	w	OH stretching
2973	m	CH_2 asymmetric stretching
2927	m	CH stretching
2883	m	CH_2 symmetric stretching
1653	vs	NO_2 asymmetric stretching
1455	w	
1424	w	CH_2 bending
1375	m	CH bending
1327	w	
1282	vs	NO_2 symmetric stretching
1207	w	
1160	m	Asymmetric oxygen bridge stretching
1118	m	Asymmetric ring stretching
1070	vs	C—O stretching in C1—O—C4′
1025	w	C—O stretching
1004	m	C—O stretching
910	w	C—O stretching
840	vs	O—NO_2 stretching
749	m	O—NO_2 deformation
692	m	O—NO_2 deformation
636	w	

[a]Abbreviations: vs: very strong; s: strong; m: medium; w: weak.

As compared with the published spectra of cellulose[10,11] or NC,[4,5] Figure 1 exhibits a better resolution. For example, the 2800–3000 cm^{-1} region exhibits two peaks for the CH_2 symmetric and asymmetric stretching modes of NC while these bands often appear unresolved in the literature in the form of a broad peak.[4,5] A similar good resolution has been noticed with several other bands of the observed spectra, as mentioned in the following paragraphs.

Figure 1 shows two very strong absorption bands due to the asymmetric and symmetric NO_2 vibration frequencies which occur, respectively, at 1653 and 1282 cm^{-1}.[12] Other absorption bands related to the nitrate functional groups are found at 840, 749 and 692 cm^{-1}.

When compared with that of cellulose,[10] the NC FTIR spectrum shows sharper and more clearly defined bands above 900 cm^{-1}, while the 740–950 cm^{-1} region, which is in principle useful for the characterization of D-glucose polymers,[13,14] is difficult to interpret due to the presence of the nitrated bands (840, 749 and 692 cm^{-1}) which mask the weak CH vibration bands of the ring. The absorption bands at about 940 and 760 cm^{-1} are typical of the α-(1 → 4)-D-glycosidic linkages,[13] and are also difficult to observe with NC.

The intensity of the OH stretching vibration bands, centered at 3315 and 3512 cm^{-1}, is small and these bands are shifted to higher frequencies than they are in the cellulose spectrum.[11,15] Typically, the OH peak location is related to the strength of the hydrogen bond involved and the stronger the hydrogen bond, the lower the frequency of the OH band.[16] This observation means that the OH groups of NC are involved in weaker hydrogen bonds than they are in pure cellulose.

No variation in the frequency of the bands assigned to the OH stretching mode was observed as a function of the nitrogen content of NC in agreement with a previous study by Broadman and Devine[17] who demonstrated that OH bands in NC appear at the same frequency for nitrogen contents above 12.5%. Similar observations have been made by different authors using a variety of techniques. Miles[1] reported, in an X-ray study of NC, that the interchain distance increases with the degree of substitution up to a nitrogen content of 12.8% N which corresponds to an average of 2.51 nitrate ester groups per glucose residue. At this point, a pattern characteristic of cellulose trinitrate appears. Clark and Stephenson[18] studied the distribution of nitrate ester groups of a series of NC by nuclear magnetic resonance spectroscopy: ^{13}C NMR spectra provide a statistical model of the sequence distribution of NO_2 groups. They showed that the NC chain is composed of blocks of fully substituted residues separated by short blocks made of residues of a lower degree of substitution. Thus, the probability to find an OH group to form a hydrogen bond is small in highly nitrated NC. Spurlin also[19] suggested that the chain in a lower nitrogen content NC is regular and offers a high probability that OH neighboring groups will form hydrogen bonds. In contrast, a NC chain with a high nitrogen content does not allow the formation of a large number of hydrogen bonds, but it also possesses a regular structure and allows van der Waals forces to exist between nitrate ester groups in neighboring chains. The NC samples investigated in this study have a nitrogen content higher than 12.6% which implies that the amount of OH groups per glucose unit is smaller than 0.55. Therefore, weak OH interactions and strong van der Waals interactions are likely to occur between these NC chains.

The CH stretching region (2800–3000 cm^{-1}) of Figure 1 is characterized by three bands of medium intensity near 2883, 2927, and 2973 cm^{-1}. Tsuboi[20] observed three bands in this region for flax fibers and assigned the two parallel bands at 2851 and 2967 cm^{-1} to the symmetric and asymmetric CH_2 stretching frequencies, respectively. Liang and Marchessault also[11] assigned the 2853 cm^{-1} band of ramie and valonia celluloses to the CH_2 symmetric stretching mode and the 2945 cm^{-1} band to the CH_2 asymmetric stretching mode, in agreement with expectations for this kind of compounds.[21] However, they noticed that one of these bands has a perpendicular polarization direction. In agreement with the observations mentioned above, Cael et al.[15] calculated, with a normal coordinate analysis of cellulose I, frequencies for the CH_2 symmetric and asymmetric stretching modes at 2868 and 2961 cm^{-1}, respectively.

For various nitrated polysaccharides including nitrocellulose, several authors have suggested assignments of the 2800–3000 cm^{-1} band region. Dawoud and Marawan[22] noticed that a number of bands near 2850, 2920, and 2970 cm^{-1} are present in the spectra of most of the nitrated polysaccharides and assigned them to the CH stretching mode. Shukla et al.[23] assigned the frequency bands of collodion at 2860 and 2930 cm^{-1} to the same vibrational mode. In contrast, Eisenreich and Pfeil[5] assigned the 2925 and 2970 cm^{-1} bands of NC to the symmetric and asymmetric CH_2 stretching modes.

Based on the normal coordinate analysis of the cellulose I[15] and IR studies of cellulose mentioned above,[10,11,20] we have assigned the 2883 and 2973 cm^{-1} bands of the FTIR spectra to the CH_2 stretching mode of nitrocellulose and the 2927 cm^{-1} band to the CH stretching mode.

Other bands assigned to the CH vibration mode of cellulose and polysaccharides are usually observed in the 1200–1400 cm^{-1} region. Shukla et al.[23] assigned the 1158, 1200, and 1375 cm^{-1} bands in the IR spectrum of collodion to CH in-plane bending modes. In the case of cellulose, Liang and Marchessault[10] observed these bands at 1282 and 1374 cm^{-1} and assigned them to the CH bending mode of the

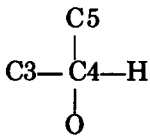

groups along the direction of the chain.

In Figure 1, we can also notice various bands in this region but the very strong 1282 cm^{-1} band is mainly due to the NO_2 vibration. However, a band of medium intensity is observed at 1375 cm^{-1} which can be assigned to the CH bending mode.

In the 1000–1200 cm^{-1}, a strong IR band is observed at 1160 cm^{-1}. The same band is also observed in IR spectra of cellulose at 1162 cm^{-1},[10] and of collodion at 1158 cm^{-1}.[23] This band has been found in most polysaccharides and is believed to be characteristic of the ring structure, although its assignment has been a matter of controversy. Segal et al.[24] have tentatively suggested that it could be related to a coupled vibration involving C—O stretching and C—OH bending modes. In contrast, Liang and Marchessault[10] considered that it could be due to the asymmetric stretching of the C1—O—C4′ bridge. The calculation of the potential energy distribution of the 1169 cm^{-1} band[15] shows a high degree of mixing but the interresidue glycosidic oxygen atom has a greater amplitude of vibration than the other atoms involved. Another strong band appears in this region at 1070 cm^{-1} (Fig. 1). This band, in the spectrum of native cellulose,[10] has been tentatively assigned to the C—O stretching mode in the C1—O—C4′ bridge.

As mentioned earlier, the nitrate absorption bands have a strong intensity in the 740–950 cm^{-1} region and cover most other vibration bands which may occur in this region. However, a weak band still appears near 910 cm^{-1} and is probably also associated with the ring skeleton: this absorption band is generally related to α-(1 → 4)-D-glycosidic linkages.[13]

The IR spectra of all the other NC samples investigated are similar to that shown in Figure 1.

Degradation Studies

A typical series of spectra recorded at various temperatures during the decomposition of a NCW-1262 film cast from ethyl acetate, at a heating rate of 0.5 K/min, is shown in Figure 2. This figure reveals a decrease in the intensity of the NO_2 bands (1653, 1282, and 840 cm^{-1}) and an increase of the 1740 cm^{-1} band as a function of temperature and time.

IR spectra of cotton cellulose heated in vacuum at 498 K revealed the appearance of an absorption band at 1725 cm^{-1}.[25] This band could be assigned to the C=O stretching vibration mode corresponding to both carbonyl

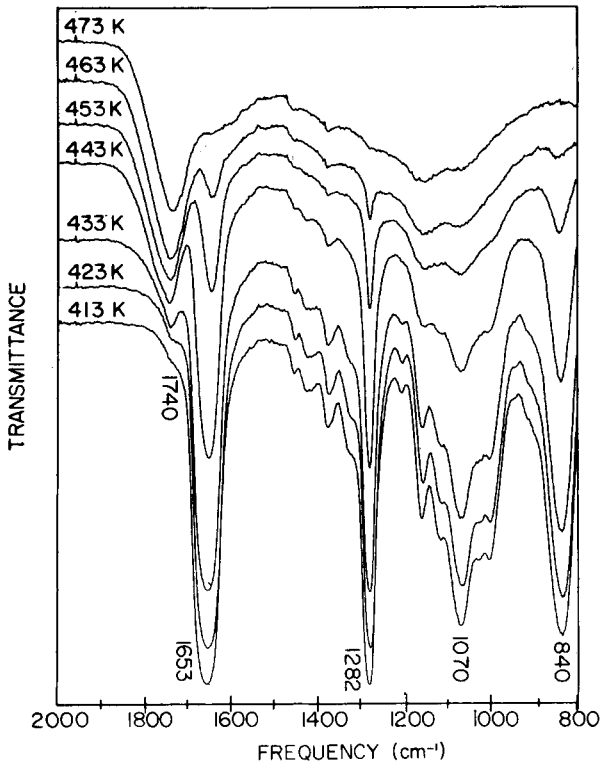

Fig. 2. FTIR spectra in the 800–2000 cm^{-1} region of a NC film cast from ethyl acetate as a function of temperature at a heating rate of 0.5 K/min. (Spectra taken from thin films. The absorbances of the 1653 and 1740 cm^{-1} bands were always in the 0.2–0.7 range.)

and carboxylic groups. In this study, the 1740 cm^{-1} band is also assigned to C=O stretching: this band is created by the O–NO_2 bond scission leading to the formation of aldehydes, ketones, and NO_2 radicals that catalyze the thermal degradation of NC, in agreement with the common accepted mechanism of nitrate decomposition. Also, the absorption band at 1070 cm^{-1} is still present in the spectra of Figure 2, even at a temperature of 480 K. This band was assigned in the previous section to the C—O stretching of the COC bridge between rings, and its presence indicates that the basic structure of the carbon skeleton does not break up during the decomposition. This observation agrees with those of Wolfrom et al.[2] who isolated the products of combustion of NC at low pressures. These products were identified as made of a fragmented type of oxycellulose consisting mainly of a central core of unaltered nitrated anhydro-D-glucose units flanked by altered units. This indicates that the thermal degradation of NC, which is a denitration process, does not necessarily lead to chain splitting.

Similar degradation results were obtained for all the NC films investigated (NCC and NCW types) after casting from acetone or THF, but they were slightly different for NCC films cast from ethyl acetate. For the latter samples, the temperature at which the NO_2 vibration bands are reduced to 50% of their initial intensity (T_{50}) is of 468 K as compared to 458 K for all the

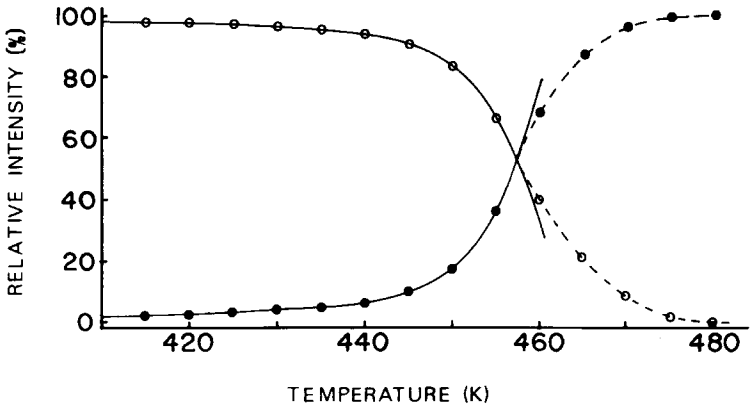

Fig. 3. 1653 (O–NO_2) –o– and 1740 cm^{-1} (C=O) –●– relative intensity as a function of temperature.

other samples, except for NCC-1274 which gives a T_{50} of 455 K. We have seen in previous studies[3,26] that the behavior of NCC-1274 is often different from that of the other NCC samples investigated.

In order to determine the kinetic parameters of NC decomposition, the fitting procedure described by Eisenreich and Pfeil[5] was used, along with a nonlinear least-squares program.[9] For this purpose, a Beer's law relationship was assumed between the functional group concentration (NO_2 and C=O) and IR absorbance. The maximum IR absorbance of the functional groups was arbitrarily chosen to be 100 (at room temperature with NO_2 and 480 K for C=O) and the minimum to be 0.

Figure 3 shows the IR relative absorbance of the 1653 cm^{-1} NO_2 and the 1740 cm^{-1} C=O bands as a function of temperature for NC degradation. It can be seen that a nonisothermal first-order autocatalytic equation [Eq. (3)] (full line) reproduces the experimental data up to 458 K (this temperature corresponds to a relative absorbance of about 55% for the NO_2 band). Above 458 K, the autocatalytic equation (solid line) deviates from the data point (dashed line) indicating that another process takes place. This analysis is in good agreement with that carried out by Eisenreich and Pfeil.[5] Curves similar to those shown in Figure 3 were obtained for all the samples studied, as well as with two other absorption bands (1282 and 840 cm^{-1}) for the NO_2 vibration mode.

Table III gives a comparison of the activation energies (E_1 and E_2) and pre-exponential factors (Z_1 and Z_2) calculated for the first-order autocatalytic reaction of all NC samples investigated, using the C=O and NO_2 vibrational groups. The values of activation energies and pre-exponential factors do not vary whatever the IR band which is used for the analysis and whatever solvent is used in casting the sample. This behavior suggests that the initial step of the decomposition, namely the breaking of the O—NO_2 bond, is the same for the monomolecular (E_1) and catalytic (E_2) reactions as was suggested by Eisenreich and Pfeil.[5]

In the literature, the dissociation energy of the O—NO_2 bond of simple nitrate esters ranges from 151 to 167 kJ/mole,[2,4,27-30] but higher values, such as those found in this study (179 kJ/mole), are expected for a solid ester.[28]

TABLE III
Kinetic Parameters of the first-order Autocatalytic Reaction

Sample	Solvent	E_1 kJ/mole	Z_1 (E17)	E_2 kJ/mole	Z_2 (E17)	Functional group[a]
NCW-1262	THF	176.7	0.479	173.9	5.19	C=O
	Ethyl acetate	179.5	0.348	174.5	6.12	C=O
	THF	176.4	0.465	172.4	5.11	NO_2
	Ethyl acetate	176.7	0.495	173.5	5.02	NO_2
NCW-1342	THF	179.2	0.198	177.2	3.84	C=O
	Ethyl acetate	180.1	0.217	178.3	3.72	C=O
	THF	180.4	0.472	175.6	3.82	NO_2
	Ethyl acetate	176.6	0.192	175.4	2.14	NO_2
NCC-1260	THF	175.8	0.409	173.2	5.02	C=O
	Ethyl acetate	179.7	0.239	178.1	3.95	C=O
	THF	175.9	0.432	172.2	5.00	NO_2
	Ethyl acetate	177.2	0.460	175.7	4.15	NO_2
NCC-1274	THF	178.7	0.327	176.4	4.19	C=O
	Ethyl acetate	179.2	0.285	176.2	3.73	C=O
	THF	178.2	0.420	176.4	4.50	NO_2
	Ethyl acetate	175.6	0.270	174.2	2.92	NO_2
NCC-1314	THF	176.8	0.597	172.3	5.32	C=O
	Ethyl acetate	180.3	0.387	174.7	6.23	C=O
	THF	176.3	0.470	171.7	5.20	NO_2
	Ethyl acetate	176.4	0.451	172.7	5.27	NO_2
NCC-1350	THF	179.6	0.213	175.8	4.32	C=O
	Ethyl acetate	180.1	0.255	178.6	4.11	C=O
	THF	180.5	0.503	175.1	4.31	NO_2
	Ethyl acetate	176.5	0.203	175.1	1.97	NO_2
NC-133 (5)		171.6	0.251	166.6	0.794	C=O
		178.3	0.631	164.9	0.631	NO_2
NC-139 (4)		185.0	21.6			C=O
		167.9	0.15			NO_2

[a] IR absorption band: C=O: 1740 cm^{-1}; NO_2: 1653 cm^{-1}.

By comparing the results of Table III with literature data,[4,5] we notice that the activation energies reported in the literature are slightly smaller than those found in this study. For a NC sample having a nitrogen content of 13.3%, Eisenreich and Pfeil[5] calculated activation energies E_1 and E_2 equal to 172 and 167 kJ/mole, respectively, using the 1740 cm^{-1} band and equal to 178 and 165 kJ/mole using the 1653 cm^{-1} band. In this study, for samples having similar nitrogen contents (NCC-1350 or NCW-1342), E_1 and E_2 are equal to 180 and 177 kJ/mole, whatever the IR absorption band used (1740 or 1653 cm^{-1}). The difference observed (about 10 kJ/mole) is probably caused by the experimental conditions used for the degradation which are slightly different. On the other hand, Phillips et al.[4] found a significant difference between the values of activation energy calculated using the 1740 cm^{-1} (E = 168 kJ/mole) or the 1653 cm^{-1} bands (E = 185 kJ/mole): the difference observed with the results presented in this study is certainly caused by the fact that Phillips et al.[4] used a simple-order kinetic equation to describe the thermal decomposition of NC, whereas an autocatalytic equation was used in this work.

For the same NC samples, similar activation energies were obtained using a thermogravimetry technique[26] and the same fitting procedure (E_1 and E_2 equal to 182 kJ/mole). The slight difference found is within the limits of experimental error.

Above 458 K, where the autocatalytic reaction equation is no longer obeyed, the experimental data can be associated with a simple reaction of either second or third order. We did not attempt to fully analyze the results in that temperature range.

Nitrogen Content

The nitrogen content of NC is commonly determined by the Lunge, the Schlosing, or the Devarda methods.[31] These methods are slow and sensitive to environmental conditions (atmospheric pressure, temperature, solubility, and vapor pressure). In the Devarda reaction, the nitrate ester is converted into an inorganic nitrate in an alkaline medium. Then, the ammonia formed is determined by titration with a strong acid standard. Alternatively, NC is decomposed with concentrated sulfuric acid in the presence of mercury and in the absence of air. Then, the nitric oxide formed is measured volumetrically.

Smeenk[31] developed a modified Devarda method for a rapid and accurate determination of the nitrogen content of NC. This technique uses 100 mg of NC and the conversion of the sample into an inorganic nitrate is completed in 10 to 15 min as compared to 1.5 h with the standard method. The subsequent Devarda reaction and the titration of the distilling ammonia take 15–20 min. The accuracy of the method is about 0.03% N.

For the same purpose, Gardon and Leopold[32] have described a microspectrophotometric method using phenoldisulphonic acid, but the conditions for the development of the color are critical. Roberts[33] also described a spectrophotometric method for the determination of nitrogen in NC, but this method is semiquantitative.

Finally, Norwitz and Chasan[34] proposed an IR procedure for the determination of the nitrogen content of raw NC and of NC in propellants. With this method, a calibration curve is drawn using the absorbance of the IR band at 1653 cm^{-1} as a function of nitrogen content. This calibration curve is then used to determine the nitrogen content of unknown NC samples. This method requires between 30 and 300 mg of sample and it shows an accuracy of about 0.05% N.

In this study, we have also used IR spectroscopy to determine the nitrogen content of NC. The method proposed does not require a calibration curve but only an internal standard. To secure good accuracy, the absorption band should be of such strength that between 30 and 60% of the light is absorbed. The Beer-Lambert equation reads:

$$\log(I_0/I) = ACd \tag{8}$$

where I_0 and I are the intensities of the incident and transmitted light, respectively, A is the extinction coefficient, C is the concentration, and d the thickness of the sample. If A is known for a given absorption band and if it is constant, then Eq. (8) can be solved for an unknown NC and used to determine its nitrogen content if the thickness of the sample is known.

TABLE IV
Determination of the Relative Extinction Coefficient of the OH Group of NC

Sample	%N	OH groups per glucose unit	$(I_0/I)_{OH}$	$(I_0/I)_{CH}$	A''
NCW-1342	13.42	0.272	75.0/57.7	75.0/31.5	1.111
NCW-1262	12.62	0.546	80.0/47.3	80.0/33.6	1.110
NCC-1260	12.60	0.552	81.0/47.3	81.0/34.2	1.107
NCC-1274	12.74	0.506	75.0/45.3	75.0/30.5	1.107
NCC-1314	13.14	0.370	78.0/54.5	78.0/32.7	1.113
NCC-1350	13.50	0.243	82.0/64.9	82.0/34.3	1.103
Average					1.109

The nitrate bands of NC at 1653 or 1282 cm^{-1} are too strong, but the OH band at 3315 cm^{-1} is much weaker and more satisfactory for this purpose. To circumvent the difficulty of measuring precisely the thickness of the sample, the ratio of two bands can be used, one of them monitoring the nitrogen content of the sample and the other being an internal reference band. The Beer-Lambert equation can then be written for the OH and for the CH bands:

$$\log(I_0/I)_{OH} = A_{OH}C_{OH}d \tag{9a}$$

$$\log(I_0/I)_{CH} = A_{CH}C_{CH}d \tag{9b}$$

Dividing these two equations one by the other, and after rearrangements, one gets:

$$[\log(I_0/I)_{OH}]/[\log(I_0/I)_{CH}] = A'C_{OH} \tag{10}$$

where:

$$A' = A_{OH}/A_{CH}C_{CH} \tag{11}$$

if we assume that C_{CH} is independent of the nitrate content. This is probably exact since the number of CH bonds per molecule is independent of the number of nitrate ester groups.

Results obtained for all six NC samples investigated are listed in Table IV. It can be seen that A' is almost constant and its average value is 1.1090. For example, if Eq. (10) is applied to the NCC-1274 sample, a concentration of 0.506 OH groups per glucose unit is found. Then, using the usual relations between degree of substitution and nitrogen content, we find that this sample has a nitrogen content of 12.71% with an average standard deviation of 0.04%. Therefore, this simple method gives accurate results which are similar to those obtained using a nitrometer. It also requires only small quantities of sample, without having to draw a calibration curve. However, this method may be less accurate for samples with nitrogen content less than 12.6%, since the position and extinction coefficient of the hydroxyl stretch absorption may then vary with the degree of hydrogen bonding in the system, and this will vary with the degree of nitration of the cellulose.

CONCLUSION

In several studies of the thermal decomposition of NC, it has been established that the gaseous products of the degradation are further reacting with the solid residue (autocatalytic reaction).

The sites where the dissociation of NC occurs are shown by arrows in the following structure formula:

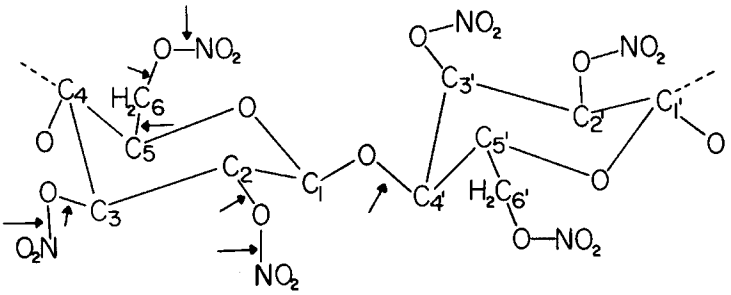

C—C, C—O and O—NO_2 bonds are likely to be disrupted, but the O—NO_2 bond is the most fragile of the three, as evidenced by the presence of NO_2 in the degradation products and the absence of NO_3 and as expected by the fact that the O—NO_2 bond dissociation requires a lower energy than the one necessary to break up a C—O bond.

Generally, it is recognized that the combustion reaction starts with the breakage of one of the O—NO_2 nitrate ester bonds. The products generated by this reaction are NO_2 and various aldehyde molecules and, apparently, the decomposition process occurs in the condensed phase or at least at the surface of the sample. These aldehydes then react with other organic compounds and NO_2 to give NO. Finally, there is an exothermic oxidation of the organic molecules by NO giving CO, CO_2, N_2, CH_4, H_2, HCHO, and H_2O.

The IR spectra shown in this study provide much experimental evidence in favor of the decomposition process described above. The presence of an absorption band at 1740 cm^{-1} in the FTIR spectra of NC at 428 K indicates the formation of a C=O band assigned to an aldehyde.

From the β-D-glucopyranose ring structure shown above with substituents in C6, C3, and C2 positions, the formation of a C=O bond can be related to the breakage of the O—NO_2 or of the O—C bonds like those found at C60—NO_2, C20—NO_2, C30—NO_2, C50—C1, or C10—C4′. Among all these possibilities, three major pathways for bond scisson can be defined: (1) conservation of the glucosidic ring structure and of the carbon skeleton if the breakage occurs at the O—NO_2 bond, (2) opening of the glucosidic ring if the scission occurs at the C50—C1 position, and (3) formation of oligomers with the C10—C4′ interring scission. The results presented in this study support the first proposal. Indeed, Figure 2 shows that the intensity of the 1740 cm^{-1} band assigned to a C=O vibrational mode increases while the intensity of the 1653, 1282, and 840 cm^{-1} bands assigned to the stretching modes of the NO_2 group decreases as a function of temperature. Furthermore, the kinetic parameters (Table III) calculated using the IR absorption bands monitoring the C=O appearance and the NO_2 loss indicate that the activation energies and the pre-exponential factors of these two processes are equal. Consequently, the

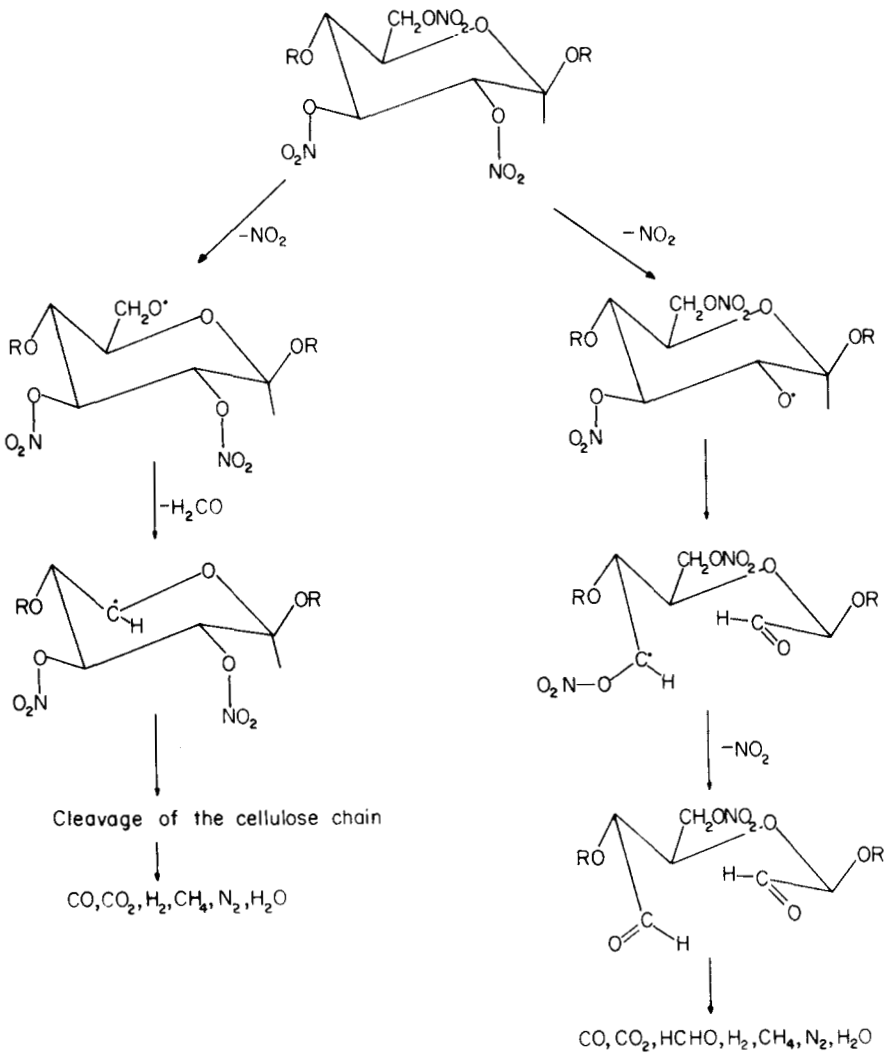

Fig. 4. Schematic of pathways to carbonyl functionalities and ring cleavage.

RO—NO_2 bond scission is responsible for the C=O formation in agreement with the literature data.

Figure 4 shows a schematic diagram, derived from the thermal studies of Wolfrom et al.,[2] describing the formation of carbonyl groups and ring cleavages occurring during the thermal decomposition of NC. In this scheme, the initial stage of the decomposition involves the RO—NO_2 bond scission, but it can occur in two different ways. The first one leads to the formation of formaldehyde following the C60—NO_2 break up and the second one involves the glucose ring opening following the C20—NO_2 or C30—NO_2 bond scission. In this study, we noticed the presence of formaldehyde which indicates that there is a breakage of the C5—C6 bond, in agreement with Shafizadeh et al.,[35] who concluded that the formaldehyde originates mainly from reactions occurring at the C6 position. However, the observation of formaldehyde and the

above conclusion concerning the C60—NO_2 scission does not exclude the second possibility shown in Figure 4 because the IR absorption bands assigned to the vibrational modes of the ring have a weak intensity and the bands assigned to the NO_2 stretching modes mask the spectral regions where the ring stretching frequencies are expected.

The results of Figure 2 show clearly that the C1—O—C4′ interring bridge is not broken up, even at a temperature of 480 K. This observation suggests that the basic carbon skeleton of NC does not change drastically during the decomposition which is in agreement with the results obtained by Wolfrom et al.,[2] who described the solid residue of the thermal degradation of a cellulose nitrate propellant as consisting of a central core of essentially unaltered anhydro-D-glucose units flanked at one or both ends by altered units.

The present study shows that NC films (prepared from solution) decompose at the same rate as NC fibers which have also been studied by IR spectroscopy[5] and have given kinetic parameters which differ little from those observed in this investigation. It appears probable that the decomposition process of NC is independent of the physical nature of the sample.

Using the same calculating procedure, the activation energies and preexponential factors determined in this study are quite similar to those obtained by thermogravimetry[26] despite the fact that the quantities measured by these two techniques are quite different: the weight losses measured in thermogravimetry represent overall changes in the molecules while the changes in the IR spectra are very specific and apply only to the particular bond or functional group being measured.

This work was supported by the Department of National Defence (Canada) (Contract N°8SD82-00150). All nitrocellulose samples were provided by the Defence Research Establishment of Valcartier. The authors thank E. Lemieux for his experimental assistance and for fruitful discussions. They also thank Dr. Michel Asselin from the Defence Research Establishment of Valcartier for his collaboration.

References

1. F. D. Miles, *Cellulose Nitrate*, Oliver and Boyd, London, 1955.
2. M. L. Wolfrom, J. H. Frazer, L. P. Kuhn, E. E. Dickey, S. M. Olin, D. O. Hoffman, R. S. Bower, A. Chaney, E. Carpenter, and P. McWain, *J. Am. Chem. Soc.*, **77**, 6573 (1955).
3. E. Lemieux and R. E. Prud'homme, *Thermochim. Acta*, **89**, 11 (1985).
4. R. W. Phillips, C. A. Orlick, and R. Steinberger, *J. Phys. Chem.*, **59**, 1034 (1955).
5. N. Eisenreich and A. Pfeil, *Thermochim. Acta*, **61**, 12 (1983).
6. M. M. Coleman and P. C. Painter, *J. Macromol. Sci. Rev. Macromol. Chem.*, **C16**, 197 (1978).
7. D. C. Cameron, J. K. Kauppinen, D. J. Moffatt, and H. H. Mantsch, *Appl. Spectrosc.*, **36**, 245 (1982).
8. N. Eisenreich, Doctorate dissertation, Technical University of Munich, 1978.
9. D. W. Marquart, *J. Soc. Indust. Appl. Math.*, **11**, 431 (1983).
10. C. Y. Liang and R. H. Marchessault, *J. Polym. Sci.*, **34**, 269 (1959).
11. C. Y. Liang and R. H. Marchessault, *J. Polym. Sci.*, **37**, 385 (1959).
12. G. Herzberg, *Infrared and Raman Spectra of Polyatomic Molecules*, Vol. 2, Van Nostrand, New York, 1964.
13. S. A. Barker, E. J. Bourne, M. Stacey, and D. H. Whiffen, *J. Chem. Soc.*, 171, (1954).
14. W. B. Neely, *Adv. Carbohyd. Chem.*, **12**, 13 (1957).
15. J. J. Cael, K. H. Gardner, J. L. Koenig, and J. Blackwell, *J. Chem. Phys.*, **62**, 1145 (1975).

16. F. Cangelosi and M. T. Shaw, *Polym. Eng. and Sci.*, **23**, 669 (1983).
17. B. W. Broadman and M. P. Devine, *J. Appl. Polym. Sci.*, **25**, 1245 (1980).
18. D. T. Clark and P. J. Stephenson, *Polymer*, **23**, 1295 (1982).
19. H. M. Spurlin, *Cellulose and Cellulose Derivates*, E. Ott and H. M. Spurlin, Eds., Interscience, New York, 1954.
20. M. Tsuboi, *J. Polym. Sci.*, **25**, 159 (1957).
21. J. J. Fox and A. E. Martin, *Proc. Roy. Soc.*, (*London*), **175A**, 208 (1940).
22. A. F. Dawoud and A. Marawan, *Carbohyd. Res.*, **26**, 65 (1973).
23. A. R. Shukla, B. P. Singh, R. K. Shukla, and D. L. Bhattacharya, *Ind. J. Pure and Appl. Phys.*, **15**, 101 (1977).
24. L. E. Segal, R. T. O'Connor, and F. V. Eggerton, *J. Am. Chem. Soc.*, **82**, 2807 (1960).
25. M. A. Moharram, T. Z. Abou El Nasr, and A. H. Nagwa, *J. Polym. Sci., Polym. Lett. Ed.*, **19**, 183 (1981).
26. J. J. Jutier and R. E. Prud'homme, *Thermochim. Acta*, **104**, 321 (1986).
27. G. Gelernter, L. C. Browning, S. R. Harris, and C. M. Mason, *J. Phys. Chem.*, **60**, 1260 (1956).
28. L. Dauerman and Y. A. Tajima, *AIAA J.*, **6**, 1468 (1968).
29. J. B. Levy, *J. Am. Chem. Soc.*, **76**, 3254 (1954).
30. J. A. Kerr, *Chem. Rev.*, **66**, 465 (1966).
31. J. G. M. M. Smeenk, *Anal. Chem.*, **46**, 302 (1974).
32. J. L. Gardon and B. Leopold, *Anal. Chem.*, **30**, 2057 (1958).
33. A. G. Roberts, *Anal. Chem.*, **21**, 813 (1949).
34. G. Norwitz and D. E. Chasan, *Talanta*, **20**, 73 (1973).
35. F. Shafizadeh and M. L. Wolfrom, *J. Am. Chem. Soc.*, **81**, 1221 (1959).

Received May 30, 1986
Accepted June 3, 1986